Aluminum composite powder as an additive in epoxy coatings for enhancement of corrosion protection of carbon steel

Meysam TOOZANDEHJANI[1], Pooria MOOZARM NIA[2], Ebrahim ABOUZARI LOTF[3], Farhad OSTOVAN[4]*, Mahnaz SHAMSHIRSAZ[1]

1. New Technologies Research Center, Amirkabir University of Technology, Tehran Polytechnic, 424 Hafez Ave., P.B.15875-4413, Tehran, Iran;
2. Section for Surface Physics and Catalysis, Department of Physics, Technic, Fysikvej, Bygning 311, Kongens Lyngby, DK-2800, Denmark;
3. Institute of Nanotechnology and Institute of Quantum Materials and Technology, Karlsruhe Institute of Technology, P.O. Box 3640, 76021 Karlsruhe, Germany;
4. Department of Materials Science and Engineering, Bandar Abbas Branch, Islamic Azad University, Bandar Abbas, Iran

Abstract: Electrochemical impedance spectroscopy (EIS) and potentiometric polarization (Tafel) tests were utilized to investigate the corrosion protection efficiency of epoxy (EP) composite coatings reinforced with aluminum powder additives deposited on carbon steel substrate. Different aluminum powders including pure aluminum (Al) and aluminum composites powders containing alumina (Al_2O_3) and carbon nanotubes (CNTs) were used as an additive filler. Various aluminum composite powders containing 2 wt.% of each CNTs and Al_2O_3 nanoparticle were synthesized using ball milling and then added into EP coating at concentration of 1 wt.%. It was found that the incorporation of formulated additive fillers improves the corrosion resistance of neat EP coating owing to enhanced barrier properties of EP composite coatings. It was also found that the barrier property of Al/CNT/Al_2O_3 additive is more significant than other additives owing to reduced particle size and certain shapes of particles as it further reduces the transport paths for penetration of corrosive environment through the coating and greatly prevents possible reactions at metal substrate/coating interface. Moreover, EP-Al/CNT/Al_2O_3 maintained one-time constant characteristic and showed the highest impedence and stability over the whole exposure time. In addition, the presence of these additives strengthens the coating, leading to further improvement of barrier property of the coating.

Key words: aluminum composite; epoxy composite coating; corrosion; electrochemical impedance spectroscopy (EIS); Tafel polarization

1 Introduction

Organic coating systems have been successfully utilized to control or mitigate the corrosion processes of the metallic substrates particularly steel materials. Among all organic coatings, epoxy resins are well developed and

Corresponding author: Farhad OSTOVAN, PhD; E-mail: f.ostovan@gmail.com; ORCID: https://orcid.org/0000-0001-8115-9715

efficiently used in the harsh corrosive environments such as marine and petrochemical industries. The main function of epoxy resins is to protect the metallic substrate through playing as a physical barrier against diffusion of corrosive agents to the surface of substrate. However, the functionality of epoxy resins is limited due to their brittle nature and presence of micro-pores. Formation of pores usually occurs during curing procedure due to evaporation of solvent which consequently reduces the hardness and barrier performance of coating [1−4].

The addition of anti-corrosive additive fillers is a common way to enhance the corrosion protection performance of epoxy resin coating without disturbing their mechanical properties. The performance of epoxy coatings is associated to the mechanism of corrosion protection of the additive fillers. These additive fillers can act under three different corrosion protection mechanisms: barrier, sacrificial and active protection [5 − 7]. Despite the advantages of these additive fillers, incorporation of these additive fillers reduces impact resistance, flexibility and transparency of epoxy coating along with increased viscosity and appearance defects [5−6]. In this regards, nano-scale additives with dimensions less than 100 nm have shown the potential to overcome many of these detriments owing to their small size and particle morphology. According to the literature, incorporation of nanoparticles as an additive filler improves integrity and durability of epoxy coating due to higher capability of nanoparticles to fill the cavities in the coating. Besides, incorporation of nanoparticles reduces coating blistering or delamination of epoxy coating and also does not disturb transparency of epoxy coating [5−8]. Oxide or carbide nanoparticles such as Al_2O_3 [7, 9], SiO_2 [10], TiO_2 [10], ZnO [3] and Fe_2O_3 [4, 11] have been already used in the organic epoxy coatings. Carbon nanotubes (CNTs) have also been successfully used as an additive filler in the epoxy coatings [12 − 13]. There are only few researches which have studied utilizing aluminium (Al) as an anticorrosive filler material in organic coatings [14 − 16]. GONZÁLEZ et al [14 − 15] have studied the effect of Al powder as a filler on the corrosion resistance of the organic epoxy coatings. Their results showed that Al pigments enhance the corrosion resistance of coating by providing a cathodic protection over the substrate. Moreover, the presence of Al pigments improves the barrier properties of coating due to the precipitation of corrosion products in the coating pores [4, 14−16].

In the present work, therefore, pure Al and aluminum composite powders containing CNTs and/or Al_2O_3 nanoparticles were synthesized and introduced into the epoxy coating as an innovative additive filler in order to enhance the corrosion protection performance of carbon steel. The corrosion protection of different epoxy coatings deposited on the surface of carbon steel was evaluated in an aqueous solution of 3.5 wt.% NaCl using EIS and Tafel polarization. Herein, the objective was to exploit the possibility of utilization of Al composite powders as a potential corrosion barrier.

2 Materials and methods

2.1 Feedstock material, substrate and reactants

Flake shape pure aluminium (Al) powder of 200 μm and 99% purity was purchased from Merck KGaA. Spherical alumina (Al_2O_3) nanoparticles with mean particle size of 200 nm were obtained from Sigma Aldrich. Multiwall carbon nanotubes (MWCNT) with purity of ~95%, outer diameter of 20−30 nm and length of 10−30 nm were purchased from Cheap Tubes Inc. In addition, epoxy resin (Epon 828), curing agent polyamide (Epikure F205), analytical grade of sodium chloride (NaCl, 99.8%) supplied from Sigma Aldrich were used. A low carbon steel was selected as a substrate.

2.2 Composite coating preparation

Initially, different powder mixtures including pure Al, Al/Al_2O_3, Al/CNT and Al/CNT/A_2O_3 were prepared using a planetary ball milling machine (Retsch Company, PM 100). In each powder mixture, constant concentrations of 2 wt.% of CNT and Al_2O_3 nanoparticles were used. The coating preparation procedure is schematically shown in Figure 1. Powders were milled for 5 h at constant rotational speed of 300 r/min while the ball to powder ratio was maintained 10: 1. The details of ball milling procedure were explained in previous works [17 − 19]. Afterward, four different powder mixtures were prepared including pure Al, Al/2 wt.% Al_2O_3, Al/2 wt.% CNT and Al/2 wt.% CNT/2 wt.% Al_2O_3 and used as an additive filler in epoxy resin, respectively.

In order to prepare epoxy coating, resin and

Figure 1 Schematic illustration of coating procedure

polyamide hardener were blended using a laboratory mixer with mixing ratio of 3: 1. 1 wt.% of each powder mixture was separately dispersed in ethanol using sonication for 20 min to prepare a homogenous powder suspension, and then directly added to epoxy resin-hardener mixture. Each nanocomposite mixture was blended for 20 min and then, it was cured in an oven at 80 ℃ for 24 h to remove the solvents. Prior applying coating, rectangular steel substrates with dimensions of 50 mm×50 mm×2 mm were mechanically ground using abrasive SiC papers up to 600 grit, degreased with acetone and finally rinsed in distilled water in order to remove rust and oxides, eliminate surface roughness and improve coating/substrate interface. Wet epoxy coatings were applied on the surface of steel substrate by using a film applicator with 50 μm thickness. The final dry thickness of each coating was measured non-destructively using Elcometer 456 at different points of coating and was about (50±5) μm. In addition, a neat epoxy coating (EP) without additive was also applied onto steel substrate as a control sample. Hereafter, the epoxy nanocomposites containing 1 wt.% of Al, Al/Al_2O_3, Al/CNT, and $Al/CNT/A_2O_3$ will be referred to as EP-Al, $EP\text{-}Al/A_2O_3$, EP-Al/CNT, and $EP\text{-}Al/CNT/A_2O_3$, respectively. The details of epoxy coatings are presented in Table 1.

2.3 Morphological and microstructural characterization

The morphology of formulated Al nanocomposites powder mixtures after ball milling at different times was examined via SEM (Hitachi S-3400, Tokyo, Japan). Dispersion uniformity of CNTs and Al_2O_3 nanoparticles during milling was observed via HRTEM (Tecnai G^2 20 S-TWIN). The particle size of nanocomposite particles was measured using MasterSizer analyzer (Malvern Instruments Ltd., Worcestershire, UK) and the mean particle size was reported. The XRD patterns of nanocomposite powders by ball milling were measured using a X'Pert highscore (PANalytical) diffractometer with a Cu-K_α radiation (λ=0.1542 nm) at 40 kV and 120 mA in the 2θ range of 20°－80° using SHIMADZU XRD-6000 detector (Shimadzu Corporation, Osaka, Japan).

2.4 Electrochemical characterization

The electrochemical tests were performed by VersaSTAT3 potentiostat (Princton Applied

Table 1 Designation of different epoxy nanocomposite coatings applied on the surface of carbon steel

Sample	Composition	Additive filler
EP	No additive	—
EP-Al	1 wt.% Al	Pure Al
$EP\text{- }Al/A_2O_3$	1 wt.% (Al/A_2O_3)	Al/2 wt.% A_2O_3
EP-Al/CNT	1 wt.% (Al/CNT)	Al/2 wt.% CNT
$EP\text{-}Al/CNT/A_2O_3$	1 wt.% ($Al/CNT/A_2O_3$)	Al/2 wt.% CNT/2 wt.% A_2O_3

Research, USA) and electrochemical corrosion protection performance of coatings was characterized by potentiometric polarization and electrochemical impedance spectroscopy (EIS). Electrochemical measurements were carried out using standard three-electrode system at room temperature. Saturated calomel electrode (SCE) and platinum (Pt) wire were used as reference electrode and counter electrode, respectively. Aqueous solution of 3.5 wt.% NaCl solution was prepared with analytical grade of sodium nitrite NaCl and Milli-Q water and used as the electrolyte solution. The working electrode was the coated substrate with an exposed working area of 1 cm^2. The EIS measurements were performed around open circuit potential (OCP) in the frequency range of $10^5 - 10^{-2}$ Hz at the amplitude of 10 mV. EIS measurements were monitored for relatively long immersion time up to 25 d at first day and every 5 d. Then, the Nyquist and bode-bode curves were plotted and quantitatively analyzed using Zview software (Version 3.1). Polarization curves were obtained from −250 mV to 250 mV at a scan rate of 0.1 mV/s vs. OCP. Additionally, three parallel samples were prepared for each sample in order to determine the reproducibility of the data. The electrochemical parameters including corrosion current density (i_{corr}), corrosion potential (E_{corr}), Tafel slops (cathodic (β_c) and anodic (β_a)), protection efficiency (P_E), polarization resistance (R_p) and corrosion rate (C_R) were extrapolated from Tafel curves. The protection efficiency, polarization resistance and corrosion rate were calculated according to equations:

$$P_E = \frac{i_{corr}(\text{uncoated}) - i_{corr}(\text{coated})}{i_{corr}(\text{uncoated})} \times 100 \text{ [20]} \quad (1)$$

$$R_p = \frac{\beta_a \beta_c}{2.303(\beta_a + \beta_c) i_{corr}} \text{ (Stern-Geary [21])} \quad (2)$$

$$C_R = \frac{k M_m i_{corr}}{\rho_m} \text{ [21]} \quad (3)$$

where k, M_m and ρ_m are constant of 3268.6 mol/A (A is the exposed surface of electrode), molar molecular weight of 56 g/mol and density of 7.86 g/cm^3.

2.5 Mechanical characterization

The nano-hardness (HN) and elasticmodulus (E) of EP coatings were measured using Micro Materials Nanotest™ indenter on the cross section of EP coatings. Nanoindentation was carried out utilizing Berkovich tip indenter at a maximum load of 250 mN. The average of 25 indentations at different locations was reported. The adhesion strength of EP coatings on steel substrates was measured by peel off test. A commercial transparent adhesive tape adhered onto the surface of EP coatings. Adhesive tape was peeled off at a 90º at rate of 10 mm/min.

3 Results and discussion

3.1 Micrographs of synthesized additive powders

Figure 2 shows SEM micrographs of different powder mixtures used as additive filler in the fabrication of the nanocomposite coatings. The morphology of as-received pure Al powders after 5 h of milling is shown in Figure 2(a). The morphology of the Al particles has preserved its initial flake shape; however, soft aluminium particles are flattened in some areas. The morphology of the Al/Al_2O_3 and Al/CNTs powders contains small and irregular shape of Al particles with smaller particle size (Figures 2(b) and (c)). Al/CNT/Al_2O_3 powders consist of equiaxed shape particles, which are distributed in certain size. The variation of particle size of each additive powder mixture is presented in Table 2. The mean size of pure Al particles is approximately 100 μm. Al/CNT/Al_2O_3 has the least particle size of 14 μm while the similar milling procedure is applied. Figure 3 shows the dispersion of CNTs and Al_2O_3 nanoparticles in each powder mixtures. CNTs and Al_2O_3 are homogenously dispersed over the Al particles in each single powder mixtures.

Table 2 Variation of particle size, crystalline size and lattice strain of pure Al, Al/Al_2O_3, Al/CNT, and Al/CNT/Al_2O_3 nanocomposites within milling process

Powder	Particle size/μm	Crystalline size/nm	Lattice strain/%
Pure Al	100±12	30±6	0.25±0.08
Al/Al_2O_3	65±7	29±5	0.41±0.05
Al/CNT	39±7	24±5	0.58±0.04
Al/CNT/Al_2O_3	14±5	10±3	0.71±0.04

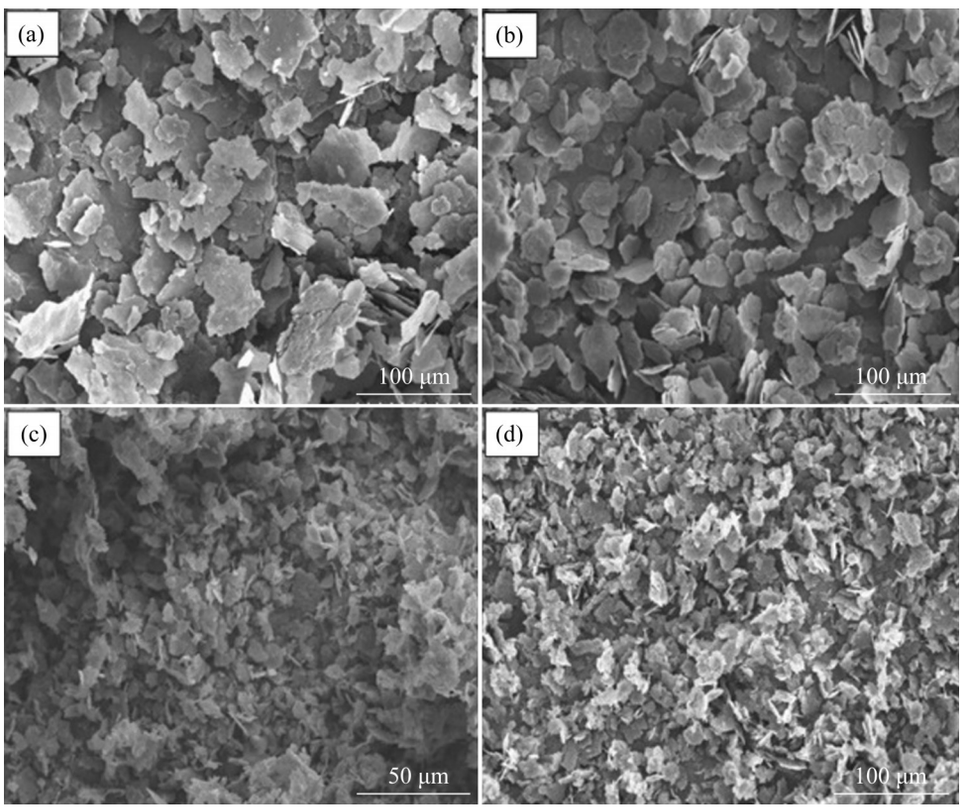

Figure 2 Morphology of (a) pure Al, (b) Al/Al_2O_3, (c)Al/CNT, and (d) $Al/CNT/Al_2O_3$ nanocomposite powders after 5 h of milling

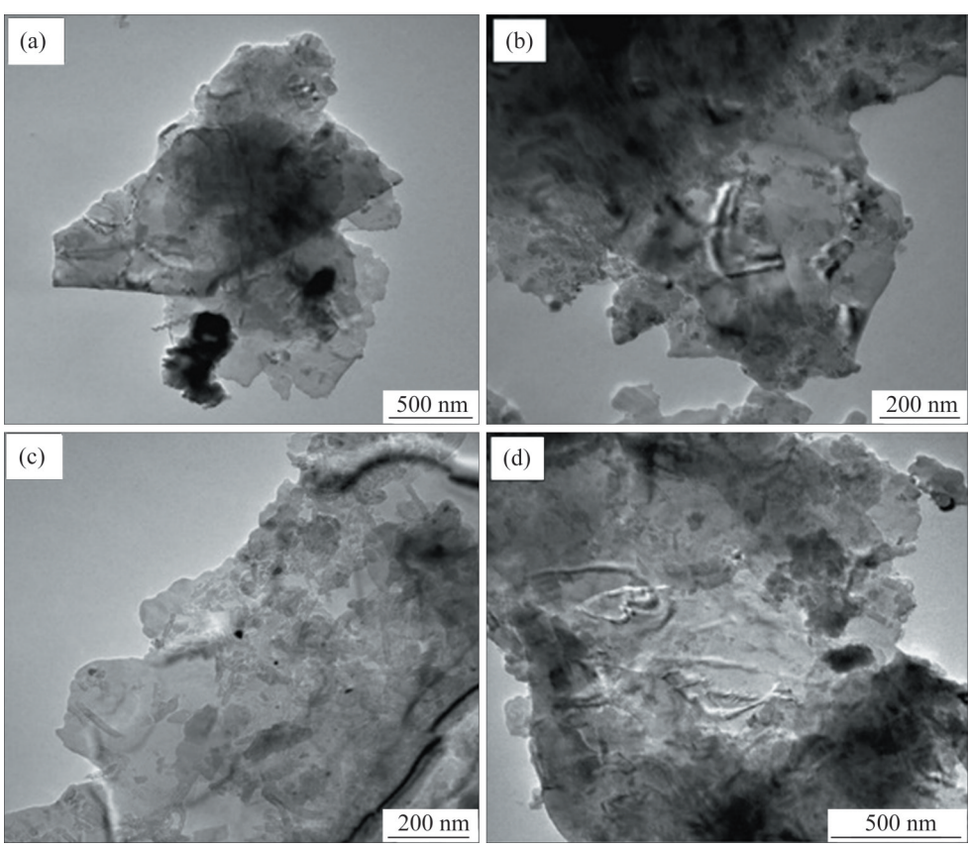

Figure 3 TEM micrographs of (a) pure Al, (b) Al/Al_2O_3, (c) Al/CNT and (d) $Al/CNT/Al_2O_3$ nanocomposite powders showing the dispersion of CNT and Al_2O_3 nanoparticles on the surface of Al particles

3.2 Electrochemical performance

3.2.1 Open-circuit potential (OCP) measurements

Before execution of electrochemical measurements, OCP measurements were performed every day for 10 min for neat EP and EP composite coatings to reach a stable potential. Figure 4 shows the OCP values of EP coatings versus immersion time in 3.5% NaCl solution. As can be seen, the OCP values of EP composite coatings shift to more positive values, representing the improvement of the corrosion resistance of EP composite coatings compared to neat EP and EP-Al/CNT/Al_2O_3 has the highest OCP value. Here, two different additives (Al_2O_3 and CNTs) are used. These composite powders with different shape and characteristics provide barrier properties and block the electrolyte diffusion toward the steel substrate. This can inhibit corrosion processes by the formation of protective layers; then, the higher OCP value is expected.

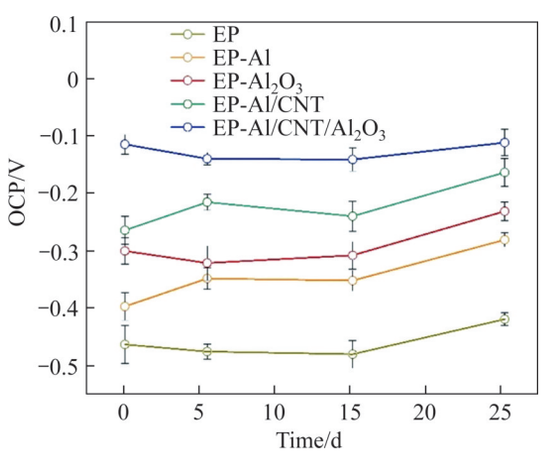

Figure 4 OCP values of EP coatings versus immersion time in 3.5% NaCl solution

3.2.2 Polarization measurements

The potentiometric polarization measurements were carried for coatings after 15 d immersion in chloride solution (3.5 wt%). Polarization curves of the neat EP and EP composite coatings during immersion are depicted in Figure 5. The electrochemical parameters including i_{corr}, E_{corr}, β_c, β_a, P_E, R_p and C_R extrapolated from Tafel curves are listed in Table 3. The bare mild steel was characterized by a high value of E_{corr} of ~−0.778 V and i_{corr} of ~10^{-2} A/cm^2, indicating a rapid electrochemical corrosion reaction. Obviously, it could be seen that corrosion process was impeded by applying the neat EP and EP composites coatings. The E_{corr} values of EP composite coatings as a measure of corrosion susceptibility were shifted toward more positive and noble values as compared to neat EP. The E_{corr} values shifted to − 0.549 V, −0.359 V, −0.277 V and −0.224 V for EP-Al, EP-Al/Al_2O_3, EP-Al/CNT and EP-Al/CNT/Al_2O_3, respectively, as compared to neat EP coating (− 0.724 V). Similarly, the calculated i_{corr} values decreased to 10^{-8} A/cm^2 for EP-Al/CNT/Al_2O_3. It meant that EP composite coatings provided superior corrosion protection performance in NaCl electrolyte compared with neat EP. Besides, β_a values of EP composite coatings were higher than neat EP that suggests the inhibition of anodic

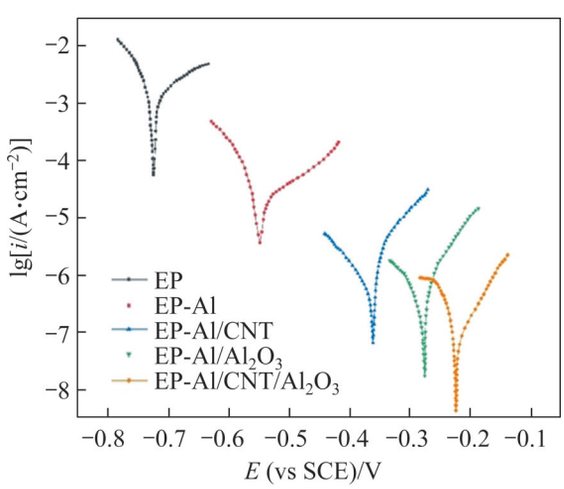

Figure 5 Polarization curves of neat epoxy and nanocomposite coatings immersed for 15 d in 3.5 wt% NaCl solution at 25 °C

Table 3 Electrochemical parameters obtained from polarization curves after 15 d immersion in 3.5% NaCl solution

Sample	E_{corr}/V	i_{corr}/(A·cm^{-2})	Tafel slopes		R_p/(MΩ·cm^{-2})	C_R/(m·a^{-1})	P_E/%
			β_c	β_a			
EP	−0.724	1.885×10^{-4}	3.22	2.77	0.002	4.600	94.0
EP-Al	−0.549	4.048×10^{-5}	2.76	2.54	0.023	1.101	97.9
EP-Al/CNT	−0.359	1.303×10^{-7}	2.06	3.50	4.639	0.013	99.3
EP-Al/ A_2O_3	−0.277	2.687×10^{-7}	3.78	3.46	2.436	0.005	99.8
EP-Al/CNT/A_2O_3	−0.224	3.171×10^{-8}	3.28	3.01	21.250	0.0007	99.9

reaction by addition of additives. In addition, depression of both cathodic and anodic branches to lower i_{corr} values was seen while the slopes did not change considerably. According to Table 3, the maximum R_p of 21.250 MΩ/cm^2 and lowest corrosion rate of 0.0007 m/a were observed in EP-Al/CNT/Al_2O_3. Meanwhile, the protection efficiency of EP-Al/CNT/Al_2O_3 (99.9%) was the highest, suggesting that the formation of more physical robust barrier and better corrosion mitigation, which reduces the corrosion rate.

3.2.3 Electrochemical impedance spectroscopy measurements (EIS)

The EIS measurements were performed to measure resistance of coatings after immersion in 3.5 wt% NaCl solution around OCP for different immersion times. Figure 6 shows the Nyquist and Bode plots of epoxy coatings at first day (day 0) and every 5 d up to 25 d of immersion in 3.5 wt.% NaCl solution around OCP. Different behaviours can be observed depending on the coating type and immersion time. It can be seen that the shape of the

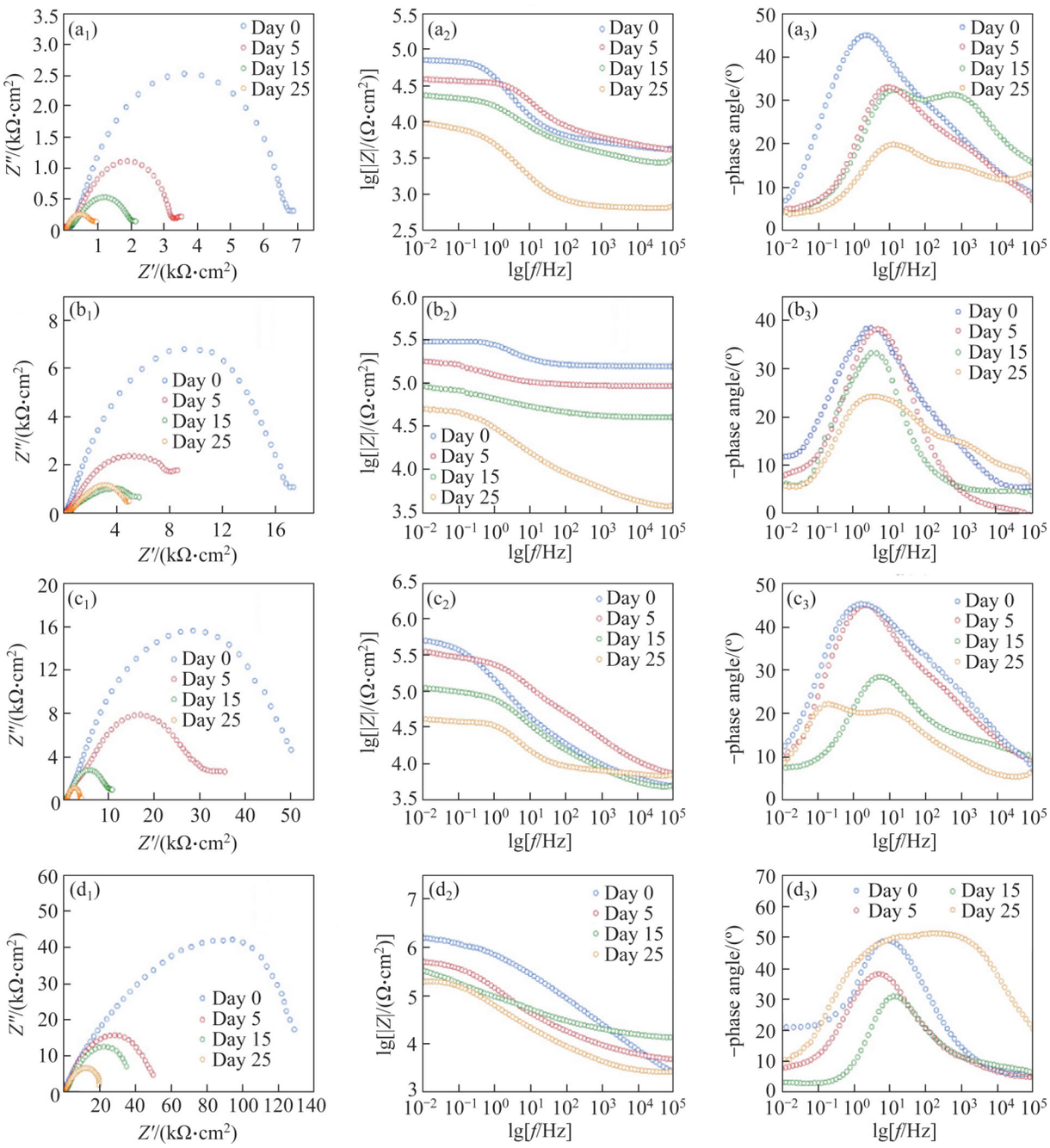

Figure 6 Representative Nyquist and Bode diagrams of EP-Al (a_1, a_2, a_3), EP-Al/Al_2O_3 (b_1, b_2, b_3), EP-Al/CNT (c_1, c_2, c_3) and EP-Al/CNT/Al_2O_3 (d_1, d_2, d_3) coatings immersed in 3.5 wt.% NaCl solutions at different immersion time up to 25 d

Nyquist diagram of coatings at different immersion time is identical with no diffusion phenomenon, but the diameters of the semi-circles, a representative of the corrosion resistance, are decreased as immersion time increased up to 25 d. As can be seen in Nyquist and Bode diagrams in Figure 6, EP-Al/CNT/Al_2O_3 is characterized by one-time constant semi-circle at different immersion time, which indicates that coating maintains good corrosion properties over time (Figure 6(d_1)). Other EP composite coatings are characterized by two-time constant semi-circle after immersion of 15 d for EP-Al (Figure 6(a_1)) and after 25 d for EP-Al/Al_2O_3 (Figure 6(b_1)) and EP-Al/CNT (Figure 6(c_1)) coatings. The two-time constant semi-circle is not well defined from the Nyquist diagrams while it can be apparently observed in Bode plots. The appearance of two-time constant semi-circle indicates the degradation of the coatings with the increase of immersion time. At this stage, electrolyte, oxygen and corrosive ions (Cl^-) can penetrate beneath the coating and reach the substrate and reduce the barrier properties of the coatings [22]. According to LIU et al [20], the appearance of a two-time constant in the middle-low frequency domain attributed to the pitting corrosion of the substrate. It is worth mentioning that the Nyquist diagrams of all coatings show flattened capacitive semi-circles. Due to the defects and flaws in the coatings, the frequency dispersion could occur, which consequently results in flattened capacitive semicircles [23].

In each EP composite coating, variations of impedance spectra with the immersion time can be clearly observed even at early days of immersion, exhibiting the evolution of the electrochemical behaviour of each coating (Figures 6(a_2) − 6(d_2)). Impedance modulus ($|Z|$) of all EP coatings steadily decreases from low frequency to high frequency as exposure time increases, revealing the gradual penetration of corrosive electrolyte into the coating and increasing porosity and electrolyte pathways. $|Z|$ values at low frequency of 0.01 Hz ($|Z|_{0.01}$) of each EP composite coatings decrease as immersion time increases up to 25 d. For example, in Al/CNT/Al_2O_3, $|Z|_{0.01}$ value slightly decreases from ~10^6 $\Omega \cdot cm^2$ at day 0 to 10^5 $\Omega \cdot cm^2$ after 25 d. The decrease in $|Z|_{0.01}$ values with immersion time indicates that coating gets defective and corrosion products are formed on the substrate; thereby the coating barrier performance reduces. By increasing immersion time, water uptake and corrosive electrolyte penetration through EP coating results in the altering dielectric properties of the coating and onset of corrosive processes on the surface of the metal substrate [14]. In addition, by increasing immersion time, the phase angle at high frequencies ($-\theta$) of EP composite coatings also slightly decreases (Figures 6(a_3) − 6(d_3)). Any defect or delamination of the EP coating in the exposure of corrosive electrolytes is reflected by decreasing θ from $-90°$ for an intact coating to 0° for bare steel [24].

The Nyquist diagrams of bare carbon steel substrate and EP nanocomposite coatings at day 0 and day 25 after exposure in 3.5 wt.% NaCl solution are depicted in Figure 7(a_1) and Figure 7(b_1), respectively. Since the dimensions of diagram of bare substrate and EP coating are too small to be discerned compared to reinforced EP coatings, the enlarged plot is depicted in the right corner of the Nyquist plots. By incorporating different additives of pure Al, Al/Al_2O_3, Al/CNT and Al/CNT/Al_2O_3, diameters of semi-circles increase, where the largest diameter was obtained when Al/CNT/Al_2O_3 was added to epoxy. The larger the time constant semicircle's diameter, the higher the polarization resistance [23, 25]. It means that EP-Al/CNT/Al_2O_3 coating provides dense, very protective and more resistance to electrochemical reactions. The similar trend can be also found after 25 d of immersion (Figure 7(b_1)). In contrast with bare carbon steel and neat EP, composite coatings have much higher resistance, indicating that nanocomposite coating provides much more prevention against possible reactions on its interface between substrate and electrolyte solution.

Figures 7(a_2) and (b_2) present the typical impedance-frequency Bode plots of bare substrate and EP coatings at day 0 and day 25. $|Z|_{0.01}$ values of EP nanocomposite coatings reinforced with pure Al, Al/Al_2O_3, Al/CNT and Al/CNT/Al_2O_3 exhibit an increase relative to the EP and bare substrate. The $|Z|_{0.01}$ values vary in the same manner as observed in Nyquist diagrams. $|Z|_{0.01}$ values of EP nanocomposite coatings increase in the order of EP-Al, EP-Al/Al_2O_3, EP-Al/CNT and EP-Al/CNT/Al_2O_3. The increase in the $|Z|_{0.01}$ value is an indicative of an increase in total corrosion resistance of the coating

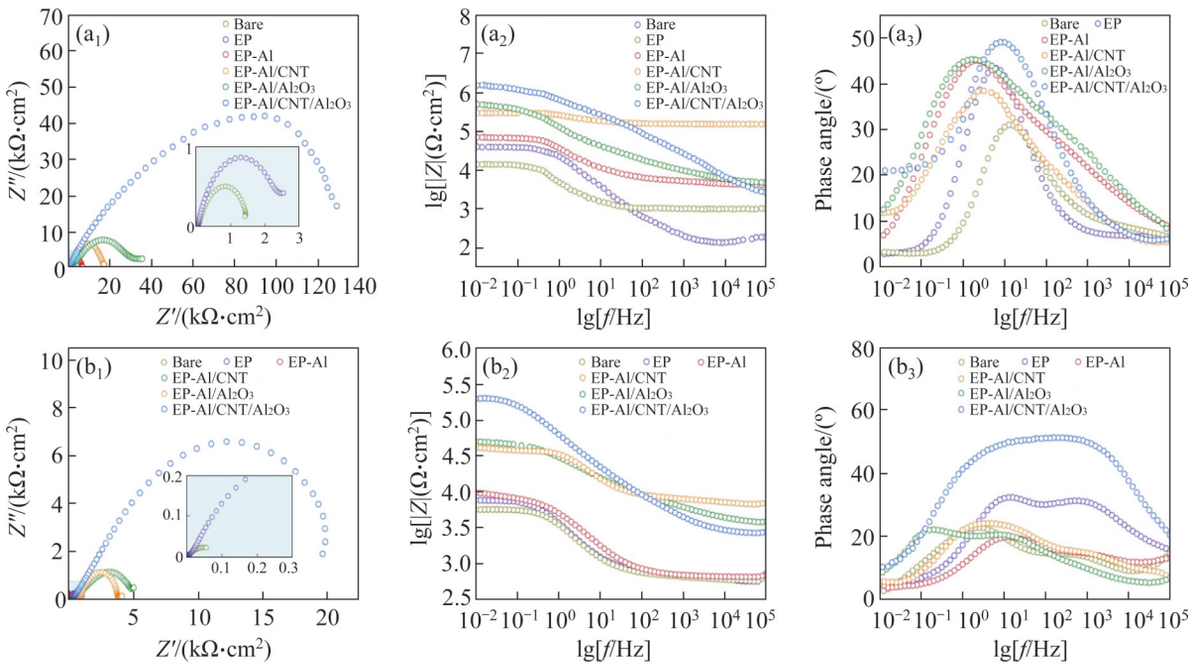

Figure 7 Representative Nyquist and Bode diagrams of different coatings immersed in 3.5 wt.% NaCl solutions at day 0 (a_1, a_2, a_3) and day 25 (b_1, b_2, b_3)

in 3.5% NaCl solution [24, 26]. $|Z|_{0.01}$ values of EP-Al/CNT/Al_2O_3 at day 0 and day 25 are much higher than other EP coatings, revealing that Al/CNT/Al_2O_3 additive obviously exerts much better corrosion protection by enhancing barrier effect. The well dispersed additives occupy the structural and pinhole porosity of neat EP and inhibit the electrolyte penetration into coating and consequently improve the barrier properties [20, 27]. Similarly, phase angle at high frequencies of EP composite coatings varies in the same order, which indicates that the addition of those additives improves epoxy coating to be denser with fewer defects (Figures 7(a_3) and (b_3)). The higher phase angle was obtained for the EP-Al/CNT/Al_2O_3 coating at the high frequency region.

In order to accurately characterize the corrosion protection performance of EP composite coatings, the experimental results were fitted with suitable electrical equivalent circuits. The equivalent circuit diagrams in Figure 8 can be proposed for simulation of the performance of EP composite coatings during immersion. In the equivalent circuits proposed, R_s, R_c, R_{pore}, R_{ct}, CPE_c and CPE_{dl} denote the solution resistance, coating resistance, microporous resistance of coating surface, charge transfer resistance, constant phase element of coating and constant phase element of double layer, respectively. The equivalent circuit (Figure 8(a)) was fitted to samples with one-time constant as the corrosive media has not reached substrate-coating interface. While, the equivalent circuit (Figure 8(b)) was fitted to samples with two-time constant in which a double layer is formed at the substrate-coating interface due to the diffusion of corrosive media into coating and reaching the interface [27].

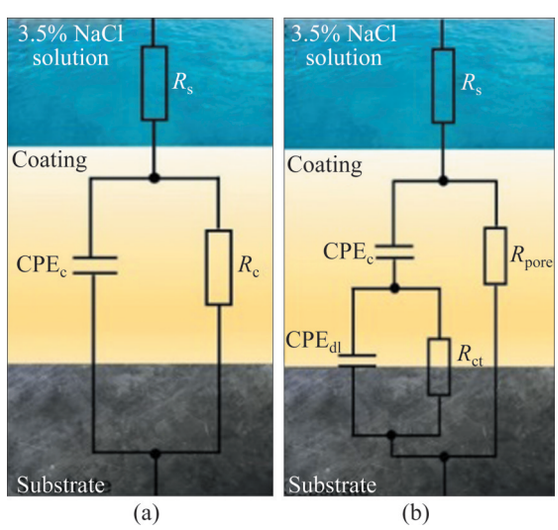

Figure 8 Equivalent electrical circuits used to fit the data achieved by the EIS analysis for one-time constant (a) and two-time constants (b)

In order to comprehend better, electrochemical parameters of EP and EP composite coatings at different immersion times were calculated based on the proposed electrical models as summarized in Table 4. Double layer capacitance characteristic was detected for neat EP after 5 d of immersion, after 10 d for EP-Al/Al_2O_3 and only 15 d for EP-Al/CNT and EP-Al/Al_2O_3, while no double layer capacitance was observed in EP-Al/CNT/Al_2O_3 even after 25 d of immersion. Both CPE_c and CPE_{dl} values of neat EP and EP composite coatings increase by extending immersion time. The increase in CPE_c and CPE_{dl} values is due to penetration of large amount corrosive electrolyte and occurrence of corrosion reactions on the steel/coating interface. Besides, the increment of CPE_{dl} shows the formation of a porous rust film on the coating [27]. CPE value of neat EP was much higher than that of EP composite coatings, which illustrates the penetaration of larger amounts of corrosive electrolyte into epoxy matrix. Among EP composite coatings, EP-Al/CNT/Al_2O_3 had the lowest CPE_c value, showing that Al/CNT/Al_2O_3 additive limits the penetration of corrosive elctrolyte by blocking pores and the defects in the coating.

According to Table 4, R_{ct} values of all samples decrease as immersion time elapses, confirming the degradation of coating and penetration of corrosive electrolyte to coating/substrate interface by increasing immersion time and resistance against the charge transfer is reduced. R_{ct} values of EP composite coatings are much higher than that of neat EP and bare steel. The incorporation of different additives restricts the penetration of the corrosive electrolyte beneath the EP coatings, resulting in less depression of R_{ct} values. The

Table 4 Impedance parameters extracted from fitting of EIS experiment of neat EP and EP composite coatings at different immersion time

Sample	Exposure time/d	R_s/ ($\Omega\cdot cm^2$)	R_c/ ($k\Omega\cdot cm^2$)	R_{pore}/ ($k\Omega\cdot cm^2$)	CPE_{coat}		CPE_{dl}		R_{ct}/ ($k\Omega\cdot cm^2$)	lg[$\|Z\|_{0.01}$/ ($k\Omega\cdot cm^2$)]
					Q_{YO}/ ($\mu\Omega^{-1}\cdot cm^{-2}\cdot s^n$)	Q_n	Q_{YO}/ ($\mu\Omega^{-1}\cdot cm^{-2}\cdot s^n$)	Q_n		
Bare substrate	0	0.01	—	11.31	—	—	138.26	0.871	10.76	4.155
	5	0.01	—	10.49	—	—	387.49	0.671	8.71	4.101
	15	0.01	—	8.86	—	—	1241.76	0.589	9.43	3.872
	25	0.01	—	6.77	—	—	2352.18	0.492	4.37	3.753
EP	0	0.01	21.89	—	62.57	0.758	—	—	—	4.608
	5	0.01	—	21.96	—	—	0.567	0.694	27.90	4.567
	15	0.01	—	17.11	—	—	1.4	0.575	19.65	4.092
	25	0.01	—	14.23	—	—	16.12	0.547	11.54	3.883
EP-Al	0	0.01	343.30	—	0.512	0.934	—	—	—	4.853
	5	0.01	267.10	—	2.24	0.724	—	—	—	4.592
	15	0.01	—	218.87	—	—	0.0561	—	213.12	4.371
	25	0.01	—	172.85	—	—	2.4	—	195.50	3.990
EP-Al/CNT	0	0.01	453.4	—	0.00512	0.943	—	—	—	5.475
	5	0.01	428.19	—	0.170	0.801	—	—	—	5.250
	15	0.01	381.33	—	8.83	0.653	—	—	—	4.966
	25	0.01	—	393.61	—	—	0.78		362.5	4.701
EP-Al/Al_2O_3	0	0.01	736.79	—	0.0067	0.951	—	—	—	5.701
	5	0.01	687.92	—	0.147	0.818	—	—	—	5.551
	15	0.01	683.18	—	3.45	0.715	—	—	—	5.053
	25	0.01	—	731.45	—	—	0.045	0.843	608.4	4.612
EP-Al/CNT/ Al_2O_3	0	0.01	1023.85	—	0.00034	0.967	—	—	—	6.192
	5	0.01	968.27	—	0.0021	0.925	—	—	—	5.701
	15	0.01	892.61	—	0.834	0.875	—	—	—	5.519
	25	0.01	831.96	—	1.8	0.901	—	—	—	5.295

increase in R_{ct} values can be attributed to the greater barrier properties of the coating in the presence of these additives [8, 27]. Meanwhile, the maximum value of R_{ct} was observed in EP-Al/Al_2O_3 (608 kΩ·cm^2) coating. Higher R_c value also illustrates that EP composite coatings are highly resistant within first 15 d except EP-Al coating with the corrosion resistance declining after 5 d of immersion. It shows that incorporation of composite additives into EP coating improves corrosion resistance. EP-Al/CNT/Al_2O_3 possessed the highest R_c values (resistance) at all immersion time studied. These electrochemical parameters are in consistent with Nyquist and Bode diagrams of neat EP and different EP composite coatings.

3.2.4 Corrosion protection mechanism

The above potentiodynamic polarization and EIS measurements indicated that the corrosion resistance of the EP composite coatings is enhanced by the addition of powder mixture additives. This improvement was more pronounced when Al/CNT/Al_2O_3 was added followed by Al/Al_2O_3, Al/CNT and pure Al particles. EP-Al/CNT/Al_2O_3 coating maintained one single time capacitive and a largest impedance modulus within 25 d of immersion compared to other coatings, which exert the best corrosion protection characteristics. The enhancement of corrosion resistance with additives, particularly Al/CNT/Al_2O_3, can be mainly attributed to the superior barrier properties of these additives. Figure 9 schematically presents the mechanism of improving the corrosion resistance performance of EP-Al/CNT/Al_2O_3 coating.

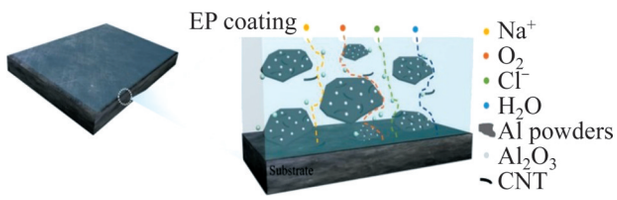

Figure 9 Schematic presentation of mechanism improving the corrosion resistance performance of EP-Al/CNT/Al_2O_3 coating

After a prolonged exposure to corrosive electrolyte, the EP coating is degraded and corrosive electrolyte gradually penetrates into coating through micro-porosities, cavities, free volumes and defects and then reaches to the substrate, leading to the substrate to be corroded. Besides, due to evaporations of solvent, significant gaps may form at the interface between the additive and the epoxy resin, leaving a channel for the penetration of corrosive media. When these additive powders are added to epoxy, additive powders occupy the vacancies in the epoxy coating and reduce the amount of surface porosities in the coating matrix as also reported earlier [21 − 22, 28]. Very rough Al/CNT/Al_2O_3 additives having less particle size and certain shape (Figure 1) provide longer diffusion paths for penetration of corrosive electrolyte beneath the EP coating and delay the corrosion process as also reported by POURHASHEM et al [29]. Besides, EP-Al/CNT/Al_2O_3 coating combines the corrosion protection advantages of both CNTs and Al_2O_3 nanoparticles. Thus, Al/CNT/Al_2O_3 additive effectively improves the corrosion protection of EP composite coating. The mild enhancement in the corrosion resistance of the EP-Al/CNT and EP-Al/Al_2O_3 coatings, might be attributed to the improper ratio of the additives to the binder resin and lower surface area of additives, which affects the interaction between the particles of the resin, as also reported in previous works [30−31].

3.3 Mechanical characterization of EP coatings

From mechanical point of view, the presence of Al/CNT, Al/Al_2O_3 and Al/CNT/Al_2O_3 additives strengthens the coating, leading to improved barrier property of the coating. The mechanical properties of the neat EP and EP composite coatings are tabulated in Table 5. It can be seen that incorporation of additives increases the hardness, elastic modulus and adhesion strength of neat EP coating. Incorporation of nanocomposite additives particularly Al/CNT/Al_2O_3 further inhibits the deformation of EP coating and crack propagation. It was also found that all EP coatings were failed and

Table 5 Mechanical properties of neat EP and EP composite coatings

Sample	*E*/GPa	Hardness/GPa	Adhesion strength/N
EP	2.31±0.1	0.18±0.06	95±4
EP-Al	3.98±0.2	0.32±0.05	110±6
EP-Al/CNT	5.25±0.6	0.48±0.07	160±5
EP-Al/A_2O_3	5.85±0.3	0.52±0.09	185±2
EP-Al/CNT/A_2O_3	6.32±0.6	0.87±0.10	245±3

lost adhesion to the substrate within pull-off stress application. The measured adhesion strengths are given in Table 5. The incorporation of composite additives enhances the adhesion of the epoxy coating. However, EP-Al/CNT/Al_2O_3 coating still shows the highest adhesion strength, which can be attributed to the good bonding of these additives to epoxy coating. High adhesion strength is necessary for a corrosion resistant performance of epoxy coatings [32−37].

4 Conclusions

Corrosion performance of EP composite coatings incorporated with pure Al, Al/Al_2O_3, Al/CNT and Al/CNT/Al_2O_3 powders as an additive filler was electrochemically analyzed using Tafel test and EIS. Electrochemical characterization outcomes revealed that corrosion protection of the neat EP coatings can be significantly improved in the presence of these additives owing to enhanced barrier properties of nanocomposite coatings. The greatest improvement was obtained when Al/CNT/Al_2O_3 additive filler was used, attributing to its smaller particle size and certain shape. EP-Al/CNT/Al_2O_3 maintained one-time constant characteristics and showed the highest impedence and stability over the whole exposure time. The presence of these aluminium powder additives provides longer diffusion paths for penetration of corrosive electrolyte through the coating and greatly prevents possible reactions at metal substrate/coating interface. From mechanical point of view, the presence of Al/CNT, Al/Al_2O_3 and Al/CNT/Al_2O_3 additives strengthens the coating, leading to improvement of barrier property of the coating.

Acknowledgements

Authors would like to thank Mr. Moein EYSHABADI for his assistant in the production of the graphical illustrations.

Contributors

Meysam TOOZANDEHJANI and Farhad OSTOVAN conceived and designed the experimental procedure. Farhad OSTOVAN supervised the entire research work. Farhad OSTOVAN and Meysam TOOZANDEHJANI carried out the experimental procedure. Pooria MOOZARM NIA provided valuable scientific advice for the entire experiment and assisted the research in analyzing data and manuscript preparation. Farhad OSTOVAN and Meysam TOOZANDEHJAN wrote the paper, while the final manuscript was revised by Ebrahim ABOUZARI LOTF and Mahnaz SHAMSHIRSAZ.

Conflict of interest

Meysam TOOZANDEHJANI, Pooria MOOZARM NIA, Ebrahim ABOUZARI LOTF, Farhad OSTOVAN and Mahnaz SHAMSHIRSAZ declare that they have no conflict of interest.

References

[1] MADHUSUDHANA A M, MOHANA K N S, HEGDE M B, et al. Functionalized graphene oxide-epoxy phenolic novolac nanocomposite: An efficient anticorrosion coating on mild steel in saline medium [J]. Advanced Composites and Hybrid Materials, 2020, 3(2): 141－155. DOI: 10.1007/s42114-020-00142-8.

[2] ZHU Qing-song, HUANG Yu-xiang, LI Yi-long, et al. Aluminum dihydric tripolyphosphate/polypyrrole-functionalized graphene oxide waterborne epoxy composite coatings for impermeability and corrosion protection performance of metals [J]. Advanced Composites and Hybrid Materials, 2021, 4(3): 780－792. DOI: 10.1007/s42114-021-00265-6.

[3] ZHANG Meng, CHEN Ping, LI Jian-chao, et al. Water-repellent and corrosion resistance properties of epoxy-resin-based slippery liquid-infused porous surface [J]. Progress in Organic Coatings, 2022, 172: 107152. DOI: 10.1016/j.porgcoat.2022.107152.

[4] MIRZAEE M, RASHIDI A, ZOLRIASATEIN A, et al. Corrosion properties of organic polymer coating reinforced two-dimensional nitride nanostructures: A comprehensive review [J]. Journal of Polymer Research, 2021, 28(2): 62. DOI: 10.1007/s10965-021-02434-z.

[5] ZHANG Meng, ZHANG Yu, CHEN Yu-cong, et al. Dual-inhibitor composite BTA/PPy/MIL-88(Fe) for active anticorrosion of epoxy resin coatings [J]. Journal of Industrial and Engineering Chemistry, 2023, 119: 660－673. DOI: 10.1016/j.jiec.2022.12.012.

[6] CHOPRA I, OLA S K, PRIYANKA, et al. Recent advances in epoxy coatings for corrosion protection of steel: Experimental and modelling approach—A review [J]. Materials Today: Proceedings, 2022, 62: 1658－1663. DOI: 10.1016/j.matpr.2022.04.659.

[7] BOOMADEVI JANAKI G, XAVIER J R. Evaluation of mechanical properties and corrosion protection performance of surface modified nano-alumina encapsulated epoxy coated mild steel [J]. Journal of Bio- and Tribo-Corrosion, 2019, 6(1): 20. DOI: 10.1007/s40735-019-0316-7.

[8] LEI Yang, ZHANG Xin-hai, LIU Qiang, et al. Skin-mimetic

assembly strategy for fabricating a transparent and highly anti-corrosive FSO-GO/epoxy nanocomposite coating [J]. Progress in Organic Coatings, 2022, 173: 107184. DOI: 10.1016/j.porgcoat.2022.107184.

[9] OLIVEIRA J D, ROCHA R C, de SOUSA GALDINO A G. Effect of Al_2O_3 particles on the adhesion, wear, and corrosion performance of epoxy coatings for protection of umbilical cables accessories for subsea oil and gas production systems [J]. Journal of Materials Research and Technology, 2019, 8(2): 1729−1736. DOI: 10.1016/j.jmrt.2018.10.016.

[10] SHI Hong-wei, LIU Fu-chun, YANG Li-hong, et al. Characterization of protective performance of epoxy reinforced with nanometer-sized TiO_2 and SiO_2 [J]. Progress in Organic Coatings, 2008, 62(4): 359−368. DOI: 10.1016/j.porgcoat.2007.11.003.

[11] SHI Xian-ming, NGUYEN T A, SUO Zhi-yong, et al. Effect of nanoparticles on the anticorrosion and mechanical properties of epoxy coating [J]. Surface and Coatings Technology, 2009, 204(3): 237 − 245. DOI: 10.1016/j.surfcoat.2009.06.048.

[12] VU C M, BACH Q V. Oxidized multiwall carbon nanotubes filled epoxy-based coating: Fabrication, anticorrosive, and mechanical characteristics [J]. Polymer Bulletin, 2021, 78(5): 2329−2339. DOI: 10.1007/s00289-020-03218-z.

[13] JEON H, PARK J, SHON M. Corrosion protection by epoxy coating containing multi-walled carbon nanotubes [J]. Journal of Industrial and Engineering Chemistry, 2013, 19(3): 849−853. DOI: 10.1016/j.jiec.2012.10.030.

[14] GONZÁLEZ S, MIRZA ROSCA I C, SOUTO R M. Investigation of the corrosion resistance characteristics of pigments in alkyd coatings on steel [J]. Progress in Organic Coatings, 2001, 43(4): 282−285. DOI: 10.1016/s0300-9440(01)00210-7.

[15] GONZÁLEZ S, CÁCERES F, FOX V, et al. Resistance of metallic substrates protected by an organic coating containing aluminum powder [J]. Progress in Organic Coatings, 2003, 46(4): 317−323. DOI: 10.1016/s0300-9440(03)00021-3.

[16] SHOURGESHTY M, ALIOFKHAZRAEI M, KARIMZADEH A, et al. Corrosion and wear properties of Zn-Ni and Zn-Ni-Al_2O_3 multilayer electrodeposited coatings [J]. Materials Research Express, 2017, 4(9): 096406. DOI: 10.1088/2053-1591/aa87d5.

[17] OSTOVAN F, HASANZADEH E, TOOZANDEHJANI M, et al. A combined friction stir processing and ball milling route for fabrication Al5083-Al_2O_3 nanocomposite [J]. Materials Research Express, 2019, 6(6): 065012. DOI: 10.1088/2053-1591/ab0a88.

[18] OSTOVAN F, MATORI K A, TOOZANDEHJANI M, et al. Microstructural evaluation of ball-milled nano Al_2O_3 particulate-reinforced aluminum matrix composite powders [J]. International Journal of Materials Research, 2021, 106(6): 636−640. DOI: 10.3139/146.111232.

[19] TOOZANDEHJANI M, OSTOVAN F. Microstructural and mechanical characterization of CNT- and Al_2O_3-reinforced aluminum matrix nanocomposites prepared by powder metallurgy route [J]. Metallography, Microstructure, and Analysis, 2017, 6(6): 541 − 552. DOI: 10.1007/s13632-017-0395-0.

[20] LIU Shuan, GU Lin, ZHAO Hai-chao, et al. Corrosion resistance of graphene-reinforced waterborne epoxy coatings [J]. Journal of Materials Science & Technology, 2016, 32(5): 425−431. DOI: 10.1016/j.jmst.2015.12.017.

[21] WANG Chuan-xing, HAN Yu-ying, WANG Wen-xue, et al. Polyvinyl chloride/epoxy double layer powder coating enhances coating adhesion and anticorrosion protection of substrate [J]. Progress in Organic Coatings, 2021, 158: 106335. DOI: 10.1016/j.porgcoat.2021.106335.

[22] XIA Yun-qing, HE Yi, CHEN Chun-lin, et al. MoS_2 nanosheets modified SiO_2 to enhance the anticorrosive and mechanical performance of epoxy coating [J]. Progress in Organic Coatings, 2019, 132: 316 − 327. DOI: 10.1016/j.porgcoat.2019.04.002.

[23] XIE Yu-hui, CHEN Ming-zhi, XIE De-long, et al. A fast, low temperature zinc phosphate coating on steel accelerated by graphene oxide [J]. Corrosion Science, 2017, 128: 1−8. DOI: 10.1016/j.corsci.2017.08.033.

[24] RAMEZANZADEH B, GHASEMI E, MAHDAVIAN M, et al. Covalently-grafted graphene oxide nanosheets to improve barrier and corrosion protection properties of polyurethane coatings [J]. Carbon, 2015, 93: 555 − 573. DOI: 10.1016/j.carbon.2015.05.094.

[25] JIANG Cong-cong, XIAO Gui-yong, ZHANG Xian, et al. Formation and corrosion resistance of a phosphate chemical conversion coating on medium carbon low alloy steel [J]. New Journal of Chemistry, 2016, 40(2): 1347 − 1353. DOI: 10.1039/C5NJ02245B.

[26] SHIBLI S M A, CHACKO F. Development of nano TiO_2-incorporated phosphate coatings on hot dip zinc surface for good paintability and corrosion resistance [J]. Applied Surface Science, 2011, 257(7): 3111 − 3117. DOI: 10.1016/j.apsusc.2010.10.125.

[27] AGHILI M, YAZDI M K, RANJBAR Z, et al. Anticorrosion performance of electro-deposited epoxy/amine functionalized graphene oxide nanocomposite coatings [J]. Corrosion Science, 2021, 179: 109143. DOI: 10.1016/j. corsci. 2020. 109143.

[28] WU Hao, CHENG Li, LIU Cheng-bao, et al. Engineering the interface in graphene oxide/epoxy composites using bio-based epoxy-graphene oxide nanomaterial to achieve superior anticorrosion performance [J]. Journal of Colloid and Interface Science, 2021, 587: 755−766. DOI: 10.1016/j.jcis.2020.11.035.

[29] POURHASHEM S, DUAN Ji-zhou, ZHOU Zi-yang, et al. Investigating the effects of chitosan solution and chitosan modified TiO_2 nanotubes on the corrosion protection performance of epoxy coatings [J]. Materials Chemistry and Physics, 2021, 270: 124751. DOI: 10.1016/j. matchemphys. 2021.124751.

[30] DHOKE S K, KHANNA A S, SINHA T J M. Effect of nano-ZnO particles on the corrosion behavior of alkyd-based waterborne coatings [J]. Progress in Organic Coatings, 2009, 64(4): 371−382. DOI: 10.1016/j.porgcoat.2008.07.023.

[31] DHOKE S K, MANGAL SINHA T J, KHANNA A S. Effect of nano-Al_2O_3 particles on the corrosion behavior of alkyd based waterborne coatings [J]. Journal of Coatings Technology and Research, 2009, 6(3): 353 − 368. DOI: 10.1007/s11998-008-9127-3.

[32] PRIYANKA D, NALINI D. Designing a corrosion resistance system using modified graphene oxide-epoxy microcapsules for enhancing the adhesion strength of the epoxy coatings [J]. Applied Surface Science Advances, 2022, 10: 100269. DOI: 10.1016/j.apsadv.2022.100269.

[33] WEI Hong-yu, XIA Jun, ZHOU Wan-lin, et al. Adhesion and cohesion of epoxy-based industrial composite coatings [J]. Composites Part B: Engineering, 2020, 193: 108035. DOI: 10.1016/j.compositesb.2020.108035.

[34] ZHANG Yong-xing, ZHAO Min, ZHANG Jiao-xia, et al. Excellent corrosion protection performance of epoxy composite coatings filled with silane functionalized silicon nitride [J]. Journal of Polymer Research, 2018, 25(5): 130. DOI: 10.1007/s10965-018-1518-2.

[35] ABDUS SAMAD U, ALAM M A, SEIKH A H, et al. Corrosion resistance performance of epoxy coatings incorporated with unmilled micro aluminium pigments [J]. Crystals, 2023, 13(4): 558. DOI: 10.3390/cryst13040558.

[36] XIAO Xin-zhe, YE Ze-quan, MENG Guo-zhe, et al. Mussel-inspired preparation of superhydrophobic mica nanosheets for long-term anticorrosion and self-healing performance of epoxy coatings [J]. Progress in Organic Coatings, 2023, 178: 107456. DOI: 10.1016/j.porgcoat.2023.107456.

[37] SHI Yan, CHEN Chong-yi, LI Yi-guo, et al. Achieving dual functional corrosion resistance for epoxy coatings under alternating hydrostatic pressure via constructing P-phenylenediamine/Ti_3C_2Tx hybrids [J]. Carbon, 2023, 201: 1048−1060. DOI: 10.1016/j.carbon.2022.09.089.